About contacts of adhesive, elasto-plastic, frictional powders

Stefan Luding

Multi Scale Mechanics (MSM), CTW, UTwente,
POBox 217, 7500 AE Enschede, Netherlands;
e-mail: s.luding@utwente.nl

Granular materials can be studied in a split-bottom ring shear cell geometry, where they show wide shear bands under slow, quasi-static, large deformation. The contact models are at the basis of their interesting collective behavior and flow-rheology as well the core ingredient for the discrete element method (DEM). The contact mechanics used involves elasto-plastic, viscous, frictional, and torque contributions.
From a single simulation only, by applying time- and (local) space-averaging, and focusing on the regions of the system that experienced considerable deformations, the critical-state yield stress (termination locus) can be obtained. It is close to linear, for non-cohesive granular materials, and nonlinear with peculiar pressure dependence, for adhesive powders – due to the nonlinear dependence of the contact adhesion on the confining forces.

Introduction

Granular materials have various applications, involving geo-technique and -physics, industrial design, mechanical- and process-engineering, as well as main challenges for physics and theoretical mechanics. Goal is to obtain (macroscopic) continuum constitutive relations that allow to predict the collective flow behavior of many particles.

DEM simulations of simple element-tests allow microscopic insight to physical experiments, as they provide, e.g., information on forces and displacements at the grain scale. DEM allows the specification of particle properties and interaction laws and then the numerical solution of Newton's equations of motion of all particles.

This paper briefly summarizes the contact laws involving elasto-plastic repulsive forces, viscous dissipative forces, frictional forces, adhesion, and rolling-resistance.

From contacts to many-particle behavior

The behavior of particulate media can be simulated either with the discrete element method (DEM) or with molecular dynamics (MD) [1–7]. MD was developed for numerical simulations of atoms and molecules while DEM is more suitable for modeling geological materials and industrial powders. We use the DEM approach, where the interaction forces between pairs of particles involve both normal and tangential direction and the resultant torques (as well as torques connected to rolling and torsion).

Since the exact calculation of the deformations of the particles is computationally too expensive, we assume that the particles remain spherical and can interpenetrate each other. Then we relate the normal interaction force to the overlapping length as $f^n = k_n\delta^n$, with a stiffness k_n and the (interpenetration) overlap δ^n that stands for the contact-deformation. The tangential force $f^t = k_t\delta^t$ is proportional to the tangential displacement of the contact points (due to both rotations and sliding) with a stiffness k_t. The tangential force is limited by Coulomb's law for sliding $f^t \leq \mu f^n$, i.e., for $\mu = 0$ one has no tangential forces at all. To account for energy

dissipation, the normal and tangential degrees of freedom are also subject to viscous, velocity dependent damping forces, for more details see [4; 8].

Adhesive Contact Model

For fine dry particles [9], not only friction is relevant, but also adhesive/cohesive/attractive contact forces, e.g., due to van der Waals forces. Due to the tiny contact area moderate forces can lead to plastic yield and irreversible deformation of the material in the vicinity of the contact. This complex behavior is modeled by introducing a variant of the linear hysteretic spring model, as introduced in Refs. [4] and briefly explained in the following.

The adhesive, elasto-plastic (hysteretic) force is introduced by allowing the normal stiffness k_n to depend on the history of the deformation. Given the plastic stiffness k_1 and the maximal elastic stiffness k_2, the un- and re-loading stiffness k^* interpolates between these two extremes. The stiffness for un-loading increases with the previous maximal overlap, $\delta_{\max}$, reached. The overlap when the unloading force reaches zero, $\delta_0 = \frac{k^*-k_1}{k^*}\delta_{\max}$, resembles the permanent plastic deformation and depends nonlinearly on the previous maximal force $f_{\max} = k_1\delta_{\max}$.

The negative forces reached by further unloading are attractive, adhesion forces, which also increase nonlinearly with the previous maximal compression force experienced. The maximal adhesion force is given by $f_{\min} = -k_c\delta_{\min}$, with $\delta_{\min} = \frac{k^*-k_1}{k^*+k_c}\delta_{\max}$.

Three physical phenomena elasticity/stiffness, plasticity and adhesion are thus quantified by three material parameters k_2, k_1, and k_c, respectively. Plasticity disappears for $k_1 = k_2$ and adhesion vanishes for $k_c = 0$. As discussed in detail in Ref. [4], for practical reasons and since extremely high forces will lead to qualitatively different contact behavior anyway, a maximal force free overlap $\delta_f = 2\phi_f a_1 a_2/(a_1 + a_2)$, was defined (with an empirical parameter $\phi_f = 0.05$), above which k^* does not increase anymore [4] and is set to the maximal value $k^*(\delta_0 > \delta_f) = k_2$. This visco-elastic, reversible branch is referred to as "limit branch" in the following (with viscous dissipation active still). It is an over-simplification of the large-deformation regime and has some physical meaning related to multiple contacts, contact-melting, and extreme deformations, however, this is not discussed further for the sake of brevity, see Ref. [10] for details.

Parameters and scaling

Note that the contact model is reasonable for fine powders [9], with (scaled) parameters given below. Before scaling, however, the parameters are arbitrary and we just use spherical particles with density $\rho = 2000\,\mathrm{kg/m^3} = 2\,\mathrm{g/cm^3}$, an average size of $a_0 = 1.1\,\mathrm{mm}$, and the width of the homogeneous size-distribution (with $a_{\min}/a_{\max} = 1/2$) is $1 - \mathcal{A} = 1 - \langle a\rangle^2/\langle a^2\rangle = 0.18922$.

The un-scaled stiffness parameters of the model are the maximal normal stiffness $k_2 = 500\,\mathrm{N/m}$, the plastic stiffness $k_1/k_2 = 1/5$, and the tangential stiffness $k_t/k_2 = 1/25$. The normal and tangential viscosities are $\gamma_n = 0.002\,\mathrm{kg\,s^{-1}}$ and $\gamma_t/\gamma_n = 1/4$. Note that friction is chosen artificially small, $\mu = 0.01$, in order to be able to focus on the effect of contact adhesion only. The above values represent arbitrary numbers as used in the DEM code and, e.g., corresponding to arbitrary mass-, length-, and time-units. However, as shown in Ref. [4], the dimensional numbers can be re-scaled, e.g., choosing the units $m_u = 1\,\mathrm{mg} = 10^{-6}\,\mathrm{kg}$, $x_u = 10\,\mathrm{mm} = 10^{-2}\,\mathrm{m}$, and $t_u = 1\,\mu\mathrm{s} = 10^{-6}\,\mathrm{s}$, so that the dimensional model parameters translate to $\rho = 2000\,\mathrm{kg/m^3}$ (unchanged), $a_0 = 11\,\mu\mathrm{m}$, $k_2 = 5.10^8\,\mathrm{N/m}$, and $\gamma_n = 2.10^{-3}\,\mathrm{kg\,s^{-1}}$ (unchanged), while the parameter ratios and other dimensionless numbers remain unaffected. In particular this order of particle size, for dry powders, is expected to display adhesive properties as implemented in the model [4; 7; 9].

Contact model for two particles

Even though this paper concerns quasi-static contacts, the contact model is best visualized by plotting the contact force against overlap during the collision of two particles, see Fig. 1. At

the beginning of a collision, the force increases along the k_1 branch. Even for large relative velocity, $v_{\rm rel} = 0.2\,$m/s, the force does not reach the k_2 branch, but it follows the k_1 branch up to quite high values, and then returns on the k^* branch during unloading – where k^* interpolates between k_1 and k_2 – until it reaches the negative k_c branch, which is followed during unloading until the end of the contact.

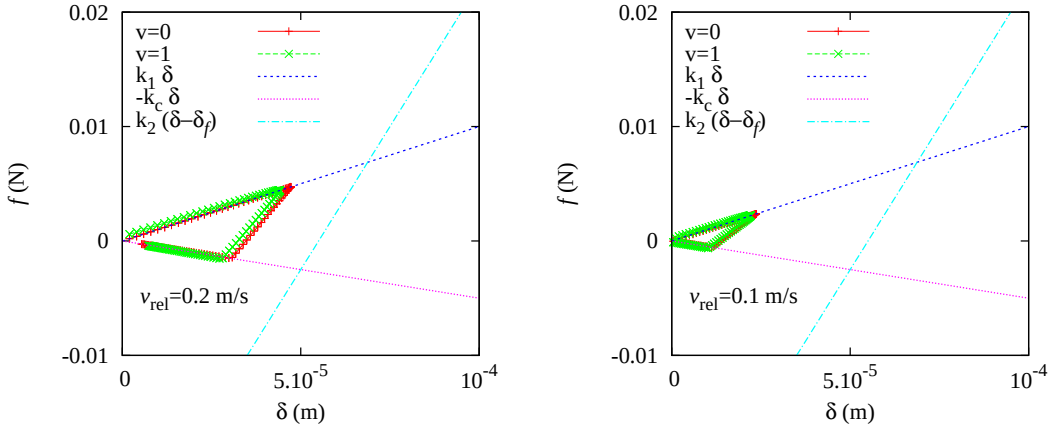

Figure 1: Contact force plotted against overlap for pair-collisions with relative velocity, $v_{\rm rel}$, as given in the panel, for two particles of average radius $a = a_0$. The green and red lines and symbols represent data for the model with (v=1) and without (v=0) normal viscosity, respectively. The three straight lines represent the plastic branch, with slope k_1, the adhesive branch, with slope $-k_c$, where $k_c/k_2 = 1/5$ is used here, and the limit-branch with slope k_2 that goes through $\delta_f = a_0\phi_f$ at zero force.

Model system geometry

The geometry of the sample for the macroscopic shear test in the split-bottom cell is described in detail in Refs. [5; 6; 11–13]. Simulations typically run for more than $50\,$s with a rotation rate $f_o = 0.01\,{\rm s}^{-1}$ of the outer cylinder, with angular velocity $\Omega_o = 2\pi f_o$. For the average of the displacement, only larger times are taken into account so that the system is examined in quasi-steady state flow conditions – disregarding the transient behavior at the onset of shear. Quasi-steady states include the possibility of very long-time relaxation effects, which can not be caught by our relatively short simulations [11].

The effect of adhesion on the shear band

Without cohesion the shear band is narrower than with cohesion – all shear-bands being rather wide close to the free surface. Very strong cohesion makes the shear-band move so rapidly inwards that it is localized (and thus narrow). Specifically, the volume fraction decays from $\nu \approx 0.66$ without cohesion to values as small as $\nu \approx 0.61$ for the strongest adhesion (in the center of the shear-band). Interestingly, in contrast to the density, the coordination number slightly increases with increasing adhesion strength, since closed contacts are less easily opened in the presence of attractive forces. The contact number density, i.e., the trace of the fabric tensor, see Refs. [5; 6] is only slightly decreasing with adhesion strength, whereas it was strongly decreasing with increasing coefficient of friction [6].

Comparing the cases with different degrees of adhesive parameters we conclude that the shear-band localisation depends strongly on adhesion.

Conclusions

Simulations of a split-bottom Couette ring shear cell with dry granular materials show perfect qualitative and good quantitative agreement with experiments. The effect of friction was studied recently, so that here the effect of contact adhesion was examined, after the elasto-plastic, adhesive contact model was introduced.

The termination locus, i.e., the maximal shear stress, $|\tau^*|$ in critical-state flow, also called critical-state yield stress, when plotted against pressure – for those parts of the system that have experienced considerable shear (displacement) – is almost linear in the absence of adhesion, corresponding to a linear Mohr-Coulomb type critical-state line (termination locus) with slope $\mu_m^* = \tan\Delta$, increasing with microscopic contact friction. A strong nonlinearity of the termination locus emerges as a consequence of the strong adhesive forces that increase nonlinearly with the confining pressure: Attractive forces are very weak for low pressure and increase considerably for larger pressure in the presence of strong contact adhesion. Saturation is observed, since the contact adhesion force cannot grow beyond a certain threshold (by construction). Therefore, due to this nonlinearity, the definition of a macroscopic cohesion (shear stress at zero normal stress) becomes questionable for low pressure levels, but is meaningful at higher confining pressure.

References

[1] P. A. Vermeer, S. Diebels, W. Ehlers, H. J. Herrmann, S. Luding, and E. Ramm, editors. *Continuous and Discontinuous Modelling of Cohesive Frictional Materials*, Berlin, 2001. Springer. Lecture Notes in Physics 568.

[2] M. Lätzel, S. Luding, and H. J. Herrmann. Macroscopic material properties from quasi-static, microscopic simulations of a two-dimensional shear-cell. *Granular Matter*, 2(3):123–135, 2000. e-print cond-mat/0003180.

[3] S. Luding. Micro-macro transition for anisotropic, frictional granular packings. *Int. J. Sol. Struct.*, 41:5821–5836, 2004.

[4] S. Luding. Cohesive frictional powders: Contact models for tension. *Granular Matter*, 10:235–246, 2008.

[5] S. Luding. Constitutive relations for the shear band evolution in granular matter under large strain. *Particuology*, 6(6):501–505, 2008.

[6] S. Luding. The effect of friction on wide shear bands. *Particulate Science and Technology*, 26(1):33–42, 2008.

[7] S. Luding and F. Alonso-Marroquin. The critical-state yield stress (termination locus) of adhesive powders from a single numerical experiment. *Granular Matter*, 13:109–119, 2011.

[8] S. Luding. Collisions & contacts between two particles. In H. J. Herrmann, J.-P. Hovi, and S. Luding, editors, *Physics of dry granular media - NATO ASI Series E350*, page 285, Dordrecht, 1998. Kluwer Academic Publishers.

[9] J. Tomas. Fundamentals of cohesive powder consolidation and flow. *Granular Matter*, 6(2/3):75–86, 2004.

[10] S. Luding, K. Manetsberger, and J. Muellers. A discrete model for long time sintering. *Journal of the Mechanics and Physics of Solids*, 53(2):455–491, 2005.

[11] J. A. Dijksman and M. van Hecke. Granular flows in split-bottom geometries. *Soft Matter*, 6:2901–2907, 2010.

[12] D. Fenistein, J. W. van de Meent, and M. van Hecke. Universal and wide shear zones in granular bulk flow. *Phys. Rev. Lett.*, 92:094301, 2004. e-print cond-mat/0310409.

[13] D. Fenistein and M. van Hecke. Kinematics – wide shear zones in granular bulk flow. *Nature*, 425(6955):256, 2003.